Sensors and Actuators B 141 (2009) 511–517

Contents lists available at ScienceDirect

Sensors and Actuators B: Chemical

journal homepage: www.elsevier.com/locate/snb

A single ZnO tetrapod-based sensor

Oleg Lupan[a,b,*], Lee Chow[a,c], Guangyu Chai[d]

[a] Department of Physics, University of Central Florida, PO Box 162385, Orlando, FL 32816-2385, United States
[b] Department of Microelectronics and Semiconductor Devices, Technical University of Moldova, 168 Stefan cel Mare Blvd., Chisinau, MD-2004, Republic of Moldova
[c] Advanced Materials Processing and Analysis Center, and Department of Mechanical, Materials, and Aerospace Engineering, University of Central Florida, PO Box 162385, Orlando, United States
[d] Apollo Technologies, Inc., 205 Waymont Court, S111, Lake Mary, FL 32746, United States

ARTICLE INFO

Article history:
Received 30 March 2009
Received in revised form 1 June 2009
Accepted 3 July 2009
Available online 15 July 2009

PACS:
78.30.Fs
78.55.Et
81.05.Dz
81.10.Dn

Keywords:
Fabrication
ZnO nanorod
ZnO tetrapod
UV sensor
Gas sensor
Zinc oxide

ABSTRACT

Transferable ZnO tetrapods were grown by an aqueous solution method. An individual ZnO tetrapod-based sensor was fabricated by in situ lift-out technique and its ultraviolet (UV) and gas sensing properties were investigated. This single tetrapod-based device responds to the UV light rapidly and showed a recovery time of about 23 s. The sensitivity of a single ZnO tetrapod sensor to oxygen concentration was also investigated. We found that when UV illumination is switched off, the oxygen chemisorption process will dominate and assists photoconductivity relaxation. Thus relaxation dynamics is strongly affected by the ambient O_2 partial pressure as described.

We also studied the response of ZnO tetrapod-based sensor in various gas environments, such as 100 ppm H_2, CO, *i*-butane, CH_4, CO_2, and SO_2 at room temperature. It is noted that ZnO tetrapod sensor is much more sensitive to H_2, *i*-butane and CO. It is demonstrated that a ZnO tetrapod exposed to both UV light and hydrogen can provide a unique integrated multiterminal architecture for novel electronic device configurations.

1. Introduction

At present, there exists emerging interest in the applications of wide-bandgap semiconductor nanomaterials. Devices based on nanoarchitectures such as nanowires, nanotubes and nanorods have attracted vast and persistent attention for a variety of applications, including detecting ultraviolet (UV) radiation, gas sensing, and detecting chemical and biological molecules [1–10]. Detection of UV radiation is important in a number of applications like flame sensing, missile plume detection, space-to-space communication, astronomy and biological research [5,9–12]. Among different wide-bandgap materials used in UV detectors, zinc oxide has a high exciton binding energy of 60 meV [13], a room temperature direct bandgap of $\Delta E_g = 3.37$ eV, and is transparent in the visible region [14]. ZnO is chemically more stable and capable of operation at much higher temperatures than Ge or Si [15]. ZnO also has an ability to operate in harsh environments and is radiation resilient [16–18]. It possesses a combination of attractive and unique optical, piezoelectrical, sensing and magnetic properties [14,19,20]. It has been demonstrated that ZnO nanorods and nanowires exhibit many unique properties associated with their shape anisotropy and high thermal and chemical stability [14,21]. Thus, the main driving force of extensive studies on micro- and nano-ZnO is the potential of new or better photonic and electronic devices that could have a huge commercial impact [22].

Several reports [5,9,11,12,23] have demonstrated that single ZnO nanorod/nanowire UV radiation and gas sensing devices have the advantages of cost-efficiency, miniaturization and low-power consumption. Due to the high aspect ratio of nanorod/nanowire, the active volume that contributes to the dark current is much smaller than that of a conventional detector. It has been suggested that, the detection sensitivity may be improved to a single photon or a single-molecular detection level [24] if the active volume can be further reduced.

Recently, it has been demonstrated that ZnO readily self-assembles into a diversity of nanocrystalline structures [19], branched nanorods [8,25], nanorod crosses [10], tetrapods [26],

* Corresponding author at: Department of Microelectronics and Semiconductor Devices, Technical University of Moldova, 168 Stefan cel Mare Blvd., Chisinau MD-2004, Republic of Moldova. Tel.: +373 22 509914; fax: +373 22 509910.
E-mail addresses: lupan@physics.ucf.edu, lupanoleg@yahoo.com (O. Lupan), chow@mail.ucf.edu (L. Chow), guangyuchai@yahoo.com (G. Chai).

0925-4005/$ – see front matter © 2009 Elsevier B.V. All rights reserved.
doi:10.1016/j.snb.2009.07.011

nanorod-based spheres and radial spherical structures [27,28], etc. These unique structures of ZnO branched rods [8,10] and ZnO tetrapods [29,30] with natural junction attracted interest as possible building blocks of novel devices. ZnO branched rods, crosses and tetrapods are used in sensor fabrication, as novel multiterminal devices. In this way, these sensors can provide several different signals at the same time. The first report of electrical contacting of single CdTe tetrapod was fabricated by Alivisatos and coworkers in 2005 [31]. Newton et al. [30] have reported the first ZnO tetrapod Schottky photodiodes in 2006 and tetrapod diodes photoresponse in 2008 [32]. Zhang et al. [33] showed that individual ZnO tetrapod multiterminal sensor can yield simultaneous multiple responses to a single input signal. Chai et al. [10], on the other hand, fabricated the first cross ZnO nanorod UV sensor in 2008. The main advantages of these types of nanostructure sensors are: (a) their multiterminal nature and (b) the junctions between different terminals, and (c) new functionality that may associate with these junctions. For example in a recent report, Huh et al. [29] suggest that the junction plays a decisive role in the electrical characteristics of the ZnO tetrapod devices. Such a sensor has an additional unique feature, which is not available in the usual nanowire-based gas sensors. Thus, the enhanced sensitivity is expected due to the junction.

So far, the ZnO tetrapods sensor reported were synthesized by chemical vapour transport technique. Here we applied the in situ lift-out technique to the zinc oxide tetrapods prepared by an aqueous solution method and report the fabrication of a sensor structure that uses the characteristics of a single ZnO tetrapod. We present in detail investigations on synthesis, sensor fabrication and on photoresponse of ZnO tetrapod electronic device. The UV induced changes in surface potential are readily manifested itself as a change in resistance of the single ZnO tetrapod. We suggest that these multiterminal devices are very sensitive. The gas sensing characteristics of this device are also described here.

2. Experimental details

This work was made possible by our recent success in synthesizing the ZnO crosses by a simple, cost-efficient and rapid aqueous solution method [25]. Transferable ZnO tetrapods were grown by a solution of zinc sulfate and ammonia in a hydrothermal reactor with glass substrate mounted inside. The system was heated at 90–98 °C for 15 min and cool down naturally without stirring.

Afterward, substrates were washed with distilled water several times and then dried in a hot air flux at 150 °C for 5 min. ZnO nanorods with different architectures were also prepared with the same procedure. This technique was also extended for various zinc oxide and tin oxide micro- and nanoarchitectures [7,10,25,27,28,34,35].

The crystalline structure of ZnO tetrapods was analyzed by X-ray diffraction (XRD) using a Rigaku "D/B max" system with CuK_α radiation ($\lambda = 1.54178$ Å). Samples were measured in a continuous scan mode with a scanning range of 10–90° (2θ) and a scanning rate of 0.01°/s. Peak positions and relative intensities of XRD were compared to values from Joint Committee on Powder Diffraction Standards (JCPDS) card for ZnO (JCPDS 036-1451).

The morphology of the ZnO nanostructures was studied using a scanning electron microscope (SEM, JEOL) and scanning transmission electron microscopy (TEM) (FEI Tecnai F30 TEM) equipped with EDS.

The current–voltage (I–V) characteristics were measured using Keithley nanovolt meter (1E−9 V to 1000 V) with an input impedance of $2.00 \times 10^8\ \Omega$ to monitor the voltage drop across the device. Also, we use Keithley current source as the power supply (range down to 1E−9 A) to run 1E−9 A through the device. The current is small enough to eliminate the Joule heating effect. Instruments were connected to a LabView programmed data acquisition to record the data in continuous mode.

The UV source used in the photosensitivity responses and current–voltage (I–V) characteristics measurements consists of an LED light source (RLT360) with a peak wavelength of 361 nm and a full width at half maximum (FWHM) of 10 nm [10]. The viewing angle of the LED is 10° and the peak power output of the LED estimated using the LED specification and the geometry of the setup was 0.7 mW. The readings were taken after a UV light was turned on as was described in detail elsewhere [10]. The photoresponses were measured at relative humidity (RH %) of 60% in a test chamber. The focused ion beam (FIB/SEM) instrument was employed to fabricate the microscale sensor. An O_2 sensitivity test was performed. The tetrapod sensor was loaded into the test chamber with electrical feed-through. After the chamber was evacuated to 5×10^{-4}–1×10^{-5} Pa and heated to 140–150 °C for 30 min to remove adsorbed oxygen from tetrapod surface. Then the chamber was cooled to room temperature (25 °C) and was introduced into dilute O_2 (200–600 ppm) balanced with N_2 gas.

The gas sensing measurements were performed by using sensor mounted in a closed quartz chamber connected to a gas flow system. The concentration of test gases was measured using pre-calibrated mass flow controller as was described elsewhere [7,8].

3. Results and discussion

3.1. Material characterization

Fig. 1 shows the X-ray diffraction (XRD) pattern for ZnO tetrapods fabricated by an aqueous solution technique on glass substrate. For all synthesis conditions, XRD data presents only peaks corresponding to hexagonal wurtzite ZnO structure with lattice constants $a = b = 0.3249$ nm, $c = 0.5206$ nm. No diffraction peaks from other impurity phase can be detected.

Scanning electron microscopy (SEM) is used to examine the surface morphology and to estimate the obtained structure uniformity on substrate. A representative SEM micrograph of the ZnO nanostructures obtained by an aqueous solution technique on glass substrate is shown in Fig. 2.

The synthesis of tetrapods ZnO nanostructures is based on solution chemistry which involves different competing kinetics as well as growth regimes [7,36–38]. Upon supersaturation, ZnO nucleates, forming the zinc blende core of growing tetrapods [36–38]. Zinc blende (ZB) and wurtzite (W) have subtle structural differences and

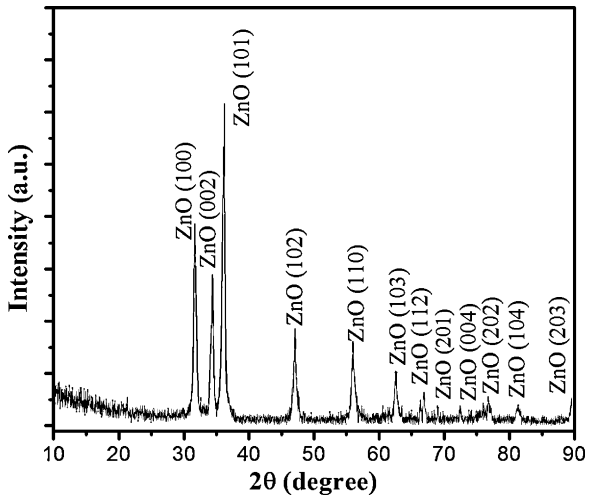

Fig. 1. XRD pattern from ZnO tetrapods on glass substrate.

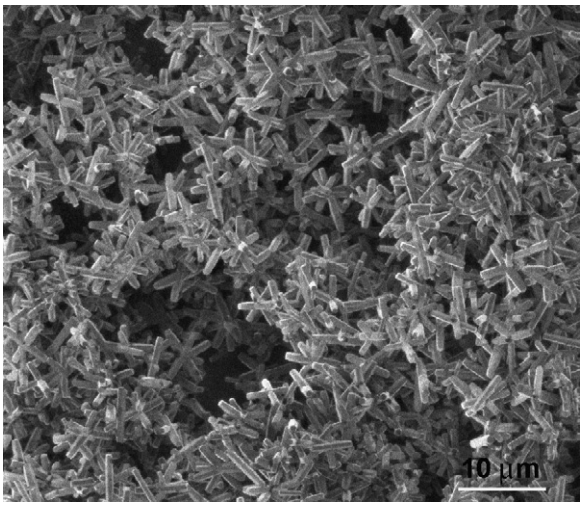

Fig. 2. Scanning electron microscope images of the ZnO micro-architectures on a glass substrate. Scale bar is 10 μm.

a small difference in the internal energies (≤20 meV/atom), which causes the well-known W–ZB polytypism [36–38]. The mechanism of growth can be explained as follows: each of four wurtzite rods/segments grows outward (Fig. 3a) from the ZB nucleus by the addition of Zn^+ and OH^- ions in the complex solution. This tetrapod structure results from nucleation in the cubic zinc blende phase with subsequent anisotropic growth in the hexagonal wurtzite phase [39,40].

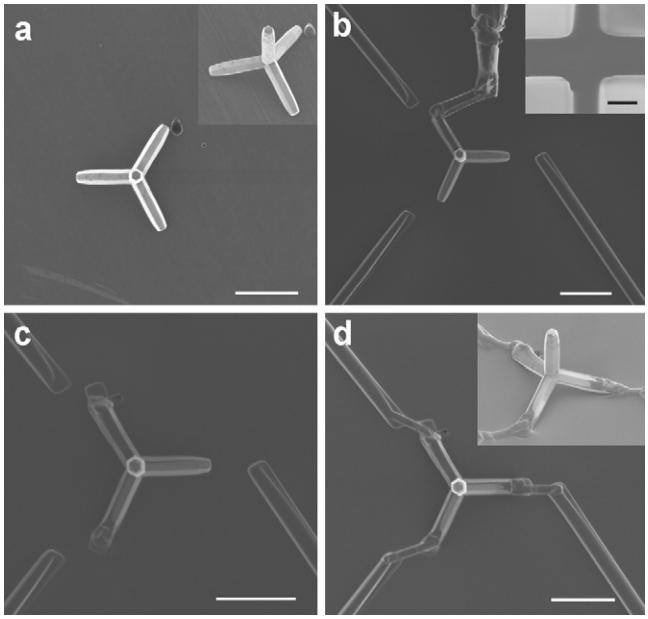

Fig. 3. Secondary electron images showing the ZnO tetrapod and the steps of the in situ lift-out fabrication procedure in the FIB/SEM system. (a) A single ZnO tetrapod on Si substrate, viewed directly from above along the *z* axis. (Insert shows side view of the ZnO tetrapod.) (b) The tungsten needle with an intermediate rod is attached to one of the legs of a ZnO tetrapod selected for sensor fabrication. It is placed next to external electrical connections. Insert is the glass substrate with Cr/Au depositions as contact electrodes (10 μm scale bar). (c) The ZnO tetrapod is placed on the substrate and next to external electrodes. (d) The ZnO tetrapod after connecting its three legs to the three external connections. Insert shows side view of a single ZnO tetrapod sensor. The scale bar is 3 μm.

3.2. Sensor fabrication and characterization

For the sensor fabrication, a SiO_2 coated Si wafer was used as intermediate substrate for tetrapods transferring. This intermediate substrate has a very low density of tetrapods which is convenient for further pick-up using in situ lift-out technique. ZnO tetrapods were transferred from the glass substrate (Fig. 2) to Si substrate (Fig. 3a) by direct contact of their faces. Silicon substrate was prepared using technique described elsewhere [25,27].

To separate an individual ZnO tetrapod for further processing an in situ FIB micromanipulator needle is used for the in situ lift-out purpose. Details on in situ lift-out procedure are described in our previous works [7–10]. We found that it is much more difficult to fabricate individual tetrapod-based devices in comparison with the single nanorod/nanowire devices. The main difficulties which have to be overcome are: (a) an individual ZnO tetrapod has to be transferable from one substrate (Fig. 2) to another (Fig. 3a); (b) the angles of tilt in the FIB chamber must be well aligned with both the initial substrate (Fig. 3a) and template substrate (Fig. 3b); (c) FIB needle with tetrapod (Fig. 3b) must be positioned very accurately with high precision in order to avoid break of the tetrapod junction. Three metal contacts were fabricated in order to connect external Au electrodes with the three legs of an individual ZnO tetrapod on the substrate (Fig. 3b). The fact that tetrapod is a 3D object makes it more difficult in general.

Currently there are no detailed illustrations of the fabrication steps in the literature related to the handling of single ZnO tetrapod. We illustrate here in detail the in situ lift-out procedures for individual tetrapod.

An in situ Kleindiek micromanipulator was mounted independent of the stage inside the FIB instrument. It permits the spatial resolution of a 1–2 nm along *z* direction and about 5–10 nm for the *x* and *y* directions. For the multiterminal device fabrication, the glass substrate was used and Cr/Au electrodes were deposited as template with external electrodes/connections (see insert in Fig. 3b). The needle used for the lift-out step was electro-polished tungsten wire.

Fig. 3a shows a single ZnO tetrapod rests on a Si substrate. We can see that in the transfer process only a very small fraction of tetrapods were transferred to the new Si substrate. This will facilitate the in situ FIB fabrication of the tetrapod devices. A side view of an individual tetrapod is shown in the insert of Fig. 3a. Closer observation (Fig. 3a, insert) reveals that the tetrapod has its three legs touching the Si substrate and one arm pointing upward and perpendicular to the substrate surface. Thus, it consists of four hexagonal rods growing from a common core at tetrahedral angles to a central junction. It can be observed that all grains of the hexagonal rods are perfectly aligned (Fig. 3). These rods have a uniform diameter along their length. The hexagonal cross-sectional radius was about 300 nm and the length of each leg was about 3000 nm. An advantage of tetrapods is that it will spontaneously orientate with one arm directed upward and the other three legs contacting the substrate. This arm may be used later as an antenna in wireless micro/nanosystems, or as an arm for surface-functionalization strategies, etc.

First the intermediate nanorod was attached to the FIB micromanipulator tip as described in our previous work [7,8]. From our past experience [7–10], we found that attachment of a single intermediate nanorod on the FIB micromanipulator tip will permit an easy pick-up of the selected tetrapod to be further handled. Next, the tip of the intermediate nanorod is brought into focus and is lowered toward the ZnO tetrapod. Let the tip positioned at one leg of the ZnO tetrapod, and connected to one leg of the ZnO tetrapod as shown in Fig. 3b. Then the FIB enhanced CVD is used to deposit 0.5 μm thickness Pt thin film to join the tip to one leg of ZnO tetrapod.

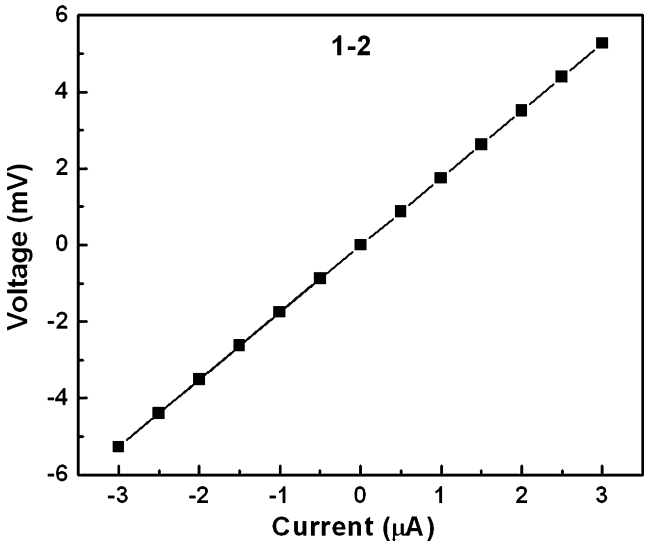

Fig. 4. *I–V* characteristics of the single ZnO tetrapod device through leg pair 1–2.

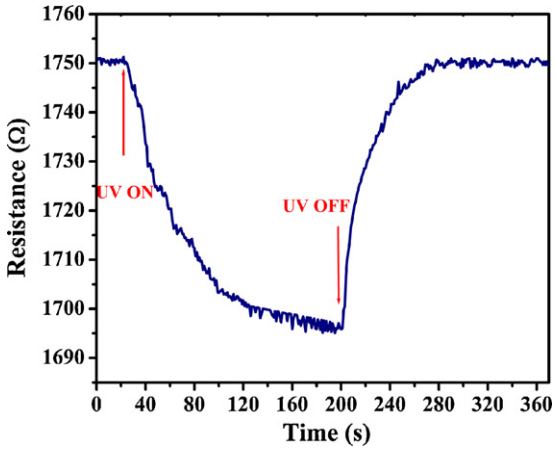

Fig. 5. The resistance change of the ZnO tetrapod-based sensor under UV irradiation. Characteristics are shown for leg pair 1–2.

In the next step, the tetrapod was transferred and then mounted with one leg to the template substrate by using FIB enhanced CVD with Pt deposition (Fig. 3c). The tetrapod is cut from an anchor point (end of intermediate point nanorod) and the needle is raised away from the substrate (Fig. 3c). Fig. 3d shows the fabricated single tetrapod-based sensor with three legs connected to external electrodes. The fourth arm is pointing upward. The main advantage of this in situ lift-out procedure is a quick verification/testing of the concept of the design of novel devices and is compatible with the fabrication of micro/nanoelectronic devices.

The current–voltage (*I–V*) characteristics (Fig. 4) showed a linear behavior between the electrodes on ZnO tetrapod legs. We have also studied *I–V* dependence through all three possible combinations up to 6 mV. Since all the connections through leg pairs displayed similar bias characteristic, only results from 1 to 2 is presented here to avoid repetition.

To study the sensitivity of a single zinc oxide tetrapod sensor to UV radiation, device was subjected to irradiation with 361 nm UV light in ambient with electrical resistance monitoring. The UV radiation applied perpendicular to the substrate surface. The background atmosphere was ambient air. It is expected that ZnO tetrapod will be sensitive to UV light of wavelength shorter than 380 nm. We also studied the spectral response of individual ZnO tetrapod sensor to light with wavelength in the range 320–500 nm.

According to results presented in Fig. 5 when the UV light was turned on, the electrical resistance shows an exponential decay with a time constant of ~45 s. This could be explained by surface process – fast desorption of the chemisorbed oxygen species at the surface of ZnO tetrapod and then by bulk process. The sensor sensitivity can be defined as the ratio of the resistivity before and after UV exposure [41].

When the UV light was turned off, the recovery of the resistance seems to be twice as fast (~23 s). This could be explained by two processes – one related to surface adsorbed species and second one to volume process as will be discussed below. We measured the resistance change between each pair of legs. The tetrapod device gives rapid responses to the UV light and showed faster recovery time.

The UV sensing phenomenon occurs because of variation in the charge carrier density. After turning on the UV light, the charge carrier density increases as a result of electron–hole (e^-–h^+) pair generation. This will reduce the resistance of ZnO tetrapod (Fig. 5). As can be observed from Fig. 5 the increase rate of the resistance is different for case when turning off the UV radiation compared to decrease rate upon UV illumination. This suggests that e^-–h^+ recombination rate in the ZnO tetrapods is slow, and this could be beneficial for further studies of photocatalytic activity. This effect was observed in several previous reports [10,42,43]. It is suggested that this rate is not only controlled by the oxygen concentration in the test chamber but also affected by the recovery of the modified surface chemistry [42]. This could be one of the main reasons of the increase rate in Fig. 5. The holes could interact with other types of negatively charged species on the ZnO surface [10,42,43].

Fabricated multiterminal sensor was exposed to UV–vis light in order to investigate spectral response. Fig. 6 shows the spectral response of the individual ZnO tetrapod-based sensor measured with the aid a Xe arc lamp dispersed by a monochromator. The light was modulated with a mechanical chopper. The relative spectral response was determined for wavelength 320–500 nm. The maximum UV photoresponse of a single ZnO tetrapod sensor was found in wavelength range from 320 nm to about 375 nm, where it remains almost constant (down to 320 nm). A sharp absorption cut-off at about 370–375 nm that corresponds to the bandgap energy of zinc oxide was reached. In addition, there was a broad absorption band around 450 nm, which could be due to the photocarriers from traps within the bandgap. According to our experimental results, the relative response is linear, which is shown in the insert in Fig. 6. All measurements are reproducible, which demonstrate suitability for UV sensor applications.

The abrupt change of the spectral response correlates with the high crystalline quality of the ZnO tetrapod as an active layer [44,45].

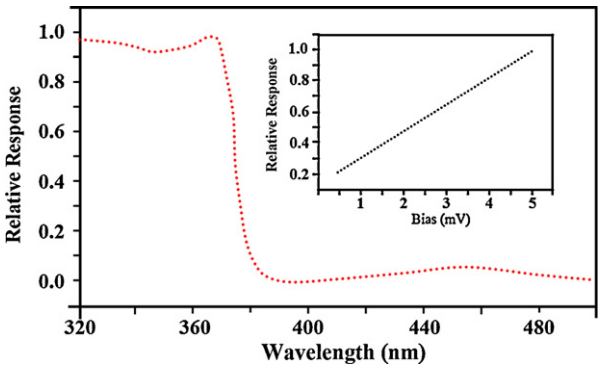

Fig. 6. Typical spectral response of the ZnO tetrapod sensor measured the identical intensity of 300 nW/cm^2. Insert shows relative response versus bias voltage.

The UV detection with a single ZnO tetrapod could be influenced by two processes as was mentioned above. First one is related to surface adsorbed species and second one to volume process. The photoresponse mechanism can be explained by the generation of the electron–hole (e^-–h^+) pairs under irradiation with photon energy higher than the bandgap. The oxygen molecules adsorbed on the ZnO surface also play an important role in UV response. Initially, the adsorbed oxygen molecules captured/deprived of the free electrons in the ZnO tetrapod form a low-conductivity depletion region and become oxygen ions (O_2^-, O^- or O^{2-}) on the surface of the ZnO tetrapod. This reduces the net carrier density in the nanowires conductance channel:

$$O_2(g) \leftrightarrow O_2(ad), \qquad O_2(ad) + e^- \rightarrow O_2^-(ad),$$
$$O_2^-(ad) + e^- \rightarrow O_2^{2-}(ad) \rightarrow 2O^-(ad),$$
$$\tfrac{1}{2}O_2 + e^- \rightarrow O^-(ad), \quad \text{or} \quad \tfrac{1}{2}O_2 + 2e^- \rightarrow O^{2-}(ad). \tag{1}$$

It is necessary to point out that the types of chemisorbed oxygen species depend strongly on the temperature. At lower temperatures, O_2^- is usually chemisorbed. However O^- and O^{2-} are commonly chemisorbed at higher temperatures, while O_2^- disappears rapidly.

Upon UV light exposure at photon energy above the bandgap (E_g), electron–hole pairs are generated ($h\nu \rightarrow e^- + h^+$) in the tetrapod legs. Holes migrate to the surface and react with negatively charged adsorbed oxygen ions on the surface and reduce depletion region:

$$h^+ + O_2^-(ad) \rightarrow O_2(g), \qquad h^+ + O^-(ad) \rightarrow \tfrac{1}{2}O_2, \quad \text{or}$$
$$2h^+ + O^{2-}(ad) \rightarrow \tfrac{1}{2}O_2. \tag{2}$$

Oxygen species is photodesorbed from the surface and unpaired. Electrons (remained from electron–hole pairs) will be free and will contribute to decrease the depletion width and the resistance of the ZnO nanoleg.

Thus conductance increases, but entire process is partially dependent on the ambient atmosphere. The quantity of the surface oxygen species on the ZnO tetrapod in vacuum is much smaller than that in the air. So in air carrier density is lower than that in vacuum due to trapping electrons by adsorbed oxygen species (Eq. (1)). Under the UV illumination the carrier density is increased because of electron–hole pairs generation and unpaired electrons (Eq. (2)). Therefore the relative change (relative response) in air is about 6% and is larger than that under vacuum (Fig. 7).

In order to verify our proposed mechanism of sensing, an O_2 sensitivity measurements/test was performed. This process suggests that an optical gating is operating within nanorod legs. It is expected that thinner nanowires may enhance the sensitivity of the device because of large surface-to-volume ratio. This could lead to the fabrication single photon detection or a single-molecular detection level [24] device, due to reduction of the effect of volume/bulk process in detection. In this case surface process due to fast desorption of the chemisorbed oxygen species at the surface of ZnO tetrapod could be decisive in photoresponse.

ZnO tetrapods have potential application as chemical gas sensors due to chemisorption. Chemisorbed gas molecules on a surface have chemical bond that will either donate or accept electrons to the ZnO [43–47].

Relative responsivity is defined as:

$$S = \frac{R_{O_2} - R_{Vacuum}}{R_{Vacuum}} \times 100\%, \tag{3}$$

where S is the relative responsivity, R_{Vacuum} the electrical resistance in vacuum (5×10^{-4} Pa), and R_{O_2} is the electrical resistance in oxygen atmosphere. Fig. 7 shows the responsivity under various oxygen pressures. This test was performed by adding oxygen (99.98%) into the sample testing chamber.

The tetrapod resistance increases monotonically with increasing O_2 at very low concentration. Each point was obtained by waiting 10 min after introducing oxygen. It is observed that the responsivity at room temperature decreases with decreasing the oxygen pressure. This is mainly due to the increasing depletion region of the electrons in ZnO [43]. Oxygen is chemisorbed to ZnO surface forming oxygen negative ions, thus leading to increase in the electrical resistance and surface charge depletion region [47].

Fig. 8 shows the gas response of the ZnO tetrapod-based multiterminal sensor to 100 ppm H_2 at the room temperature. When exposed to 100 ppm H_2, a behavior of sharp increase and then slow decrease in the gas response was observed.

When a pulse of hydrogen was introduced, the response increased sharply again, followed by a saturation region. All responses were studied for different leg pairs and we found that they are all similar to each other, therefore only results from 1 to 2 will be presented here.

Fig. 9 shows the response test of ZnO tetrapod-based sensor in various gas environments, such as 100 ppm H_2, CO, *i*-butane, CH_4, CO_2, and SO_2 at room temperature. It is noted that the response to H_2 and CO gas is significantly higher than that of the other gases. For a single ZnO tetrapod sensor the response to 100 ppm H_2 is >6 times higher than the response to 100 ppm CH_4, CO_2, and SO_2.

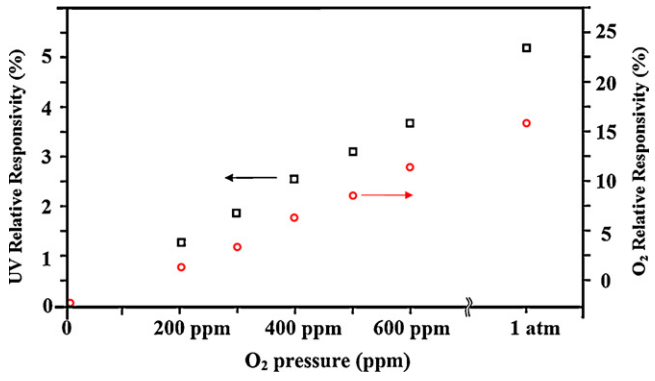

Fig. 7. Sensitivity to UV light and oxygen concentration of a single ZnO tetrapod sensor. Oxygen gas was added with N_2 as buffer gas into the chamber.

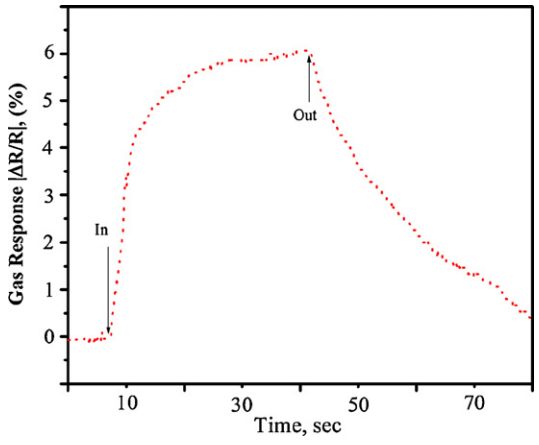

Fig. 8. Responsivity of the ZnO tetrapod sensor to 100 ppm H_2 gas at the room temperature.

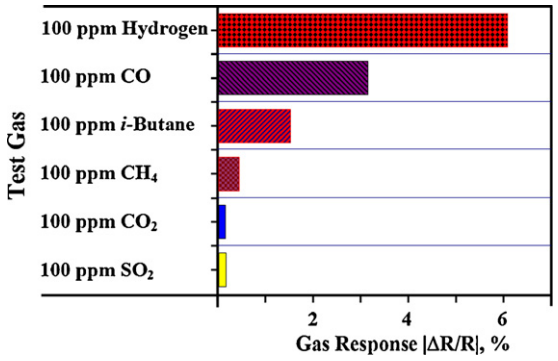

Fig. 9. Gas response of ZnO tetrapod-based sensor to different gases at 100 ppm concentration.

4. Conclusions

In conclusion, the ZnO tetrapods were synthesized by a cost-effective aqueous chemical method [25]. An in situ focused ion beam lift-out technique is developed to fabricate individual ZnO tetrapod-based UV light and gas sensor. The photoresponse of this tetrapod sensor to the 361 nm UV radiation was measured as a function of O_2 concentration from 200 ppm to 600 ppm and at 1 atm. The photoresponse mechanism is explained qualitatively on the base of adsorption and photodesorption of ambient gas molecules and bulk process. It is suggested that oxygen ions on the ZnO surface of the tetrapod influence the UV sensitivity. We conclude that, the photoresponse is dependent on the surface chemistry. A coupled ZnO tetrapod can provide a unique integrated multiterminal architecture for novel electronic device configurations.

It is suggested that oxygen ions on the surface of the ZnO tetrapod have a profound effect on UV and gas sensitivity due to the absorption of O_2 on the surface of ZnO. We have investigated this relationship by sensing UV light and O_2 gas simultaneously. This effect suggests that e–h recombination rate in the ZnO nanorod legs is relatively slow, but this could be beneficial for further studies of photocatalytic activity.

The ZnO tetrapod-based sensor was also studied in various environments, such as 100 ppm H_2, CO, *i*-butane, CH_4, CO_2, and SO_2 at room temperature. It is noted that sensor is much more sensitive to H_2, *i*-butane and CO, than to CH_4, SO_2, and CO_2.

We believe that by using ZnO tetrapod as a building unit in novel multiterminal devices, a novel multisensory structure can be developed. Such sensors will be able to avoid "false response" or can be used for different sensing information.

Acknowledgements

The financial support from Apollo Technologies, Inc., and Florida High Tech Corridor Research Program is acknowledged. The research described in this publication was partly supported by Award No. MTFP-1014B Follow-on of the Moldovan Research and Development Association (MRDA) and the U.S. Civilian Research and Development Foundation (CRDF).

References

[1] P. Kim, C.M. Lieber, Nanotube nanotweezers, Science 286 (1999) 2148–2150.
[2] Z.L. Wang, Oxide nanobelts and nanowires—growth, properties and applications, J. Nanosci. Nanotechnol. 8 (2008) 27–55.
[3] M. Law, J. Goldberger, P. Yang, Semiconductor nanowires and nanotubes, Annu. Rev. Mater. Res. 34 (2004) 83–122.
[4] A. Liu, Towards development of chemosensors and biosensors with metal-oxide-based nanowires or nanotubes, Biosens. Bioelectron. 24 (2008) 167–177.
[5] H. Kind, H. Yan, B. Messer, M. Law, P. Yang, Nanowire ultraviolet photodetectors and optical switches, Adv. Mater. 14 (2002) 158–160.
[6] X.J. Huang, Y.K. Choi, Chemical sensors based on nanostructured materials, Sens. Actuators B: Chem. 122 (2007) 659–671.
[7] O. Lupan, G. Chai, L. Chow, Novel hydrogen gas sensor based on single ZnO nanorod, Microelectron. Eng. 85 (2008) 2220–2226.
[8] O. Lupan, G. Chai, L. Chow, Fabrication of ZnO nanorod-based hydrogen gas nanosensor, Microelectron. J. 38 (2007) 1211–1216.
[9] O. Lupan, L. Chow, G. Chai, L. Chernyak, O. Lopatiuk, H. Heinrich, Focused-ion-beam fabrication of ZnO nanorod-based UV photodetector using the in-situ lift-out technique, Phys. Status Solidi A 205 (2008) 2673–2678.
[10] G. Chai, O. Lupan, L. Chow, H. Heinrich, Crossed zinc oxide nanorods for ultraviolet radiation detection, Sens. Actuators A: Phys. 150 (2) (2009) 184–187.
[11] O. Lupan, G. Chai, L. Chow, Fabrication and characterizations of ultra violet photosensor based on single ZnO nanorod, in: Technical Proceedings of the 2008 NSTI Nanotechnology Conference and Trade Show, NSTI-Nanotech, Nanotechnology, vol. 3, 2008, pp. 5–8, NanoTech-2008.
[12] J.B.K. Law, J.T.L. Thong, Simple fabrication of a ZnO nanowire photodetector with a fast photoresponse time, Appl. Phys. Lett. 88 (2006) 133114.
[13] D.G. Thomas, The exciton spectrum of zinc oxide, J. Phys. Chem. Sol. 15 (1960) 86–96.
[14] Ü. Özgür, Ya.I. Alivov, C. Liu, A. Teke, M.A. Reshchikov, S. Dogan, V. Avrutin, S.-J. Cho, H. Morkoc, A comprehensive review of ZnO materials and devices, J. Appl. Phys. 98 (2005) 041301.
[15] Y. Cui, Z. Zhong, D. Wang, W.U. Wang, C.M. Leiber, High performance silicon nanowire field effect transistors, Nano Lett. 3 (2003) 149–152.
[16] F.D. Auret, S.A. Goodman, M. Hayes, M.J. Legodi, H.A. van Laarhoven, D.C. Look, Electrical characterization of 1.8 MeV proton-bombarded ZnO, Appl. Phys. Lett. 79 (2001) 3074.
[17] A. Burlacu, V.V. Ursaki, D. Lincot, V.A. Skuratov, T. Pauporte, E. Rusu, I.M. Tiginyanu, Enhanced radiation hardness of ZnO nanorods versus bulk layers, Phys. Status Solidi (RRL)—Rapid Res. Lett. 2 (2008) 68.
[18] R.E. Peale, E.S. Flitsiyan, C. Swartz, O. Lupan, L. Chernyak, L. Chow, W.G. Vernetson, Z. Dashevsky, Neutron transmutation doping and radiation hardness for solution-grown bulk and nano-structured ZnO, in: M. Mastro, J. LaRoche, F. Ren, J.-I. Chyi, J. Kim (Eds.), Performance and Reliability of Semiconductor Devices, Mater. Res. Soc. Symp. Proc., vol. 1108, 2009 (Warrendale, PA), 1108-A05-03.
[19] Z.L. Wang, Zinc oxide nanostructures: growth, properties and applications, J. Phys.: Cond. Matter 16 (2004) R829–R858.
[20] X.D. Bai, P.X. Gao, Z.L. Wang, E.G. Wang, Dual-mode mechanical resonance of individual ZnO nanobelts, Appl. Phys. Lett. 82 (2003) 4806–4808.
[21] V.A. Karpina, V.I. Lazorenko, C.V. Lashkarev, V.D. Dobrowolski, L.I. Kopylova, V.A. Baturin, S.A. Pustovoytov, A.Ju. Karpenko, S.A. Eremin, P.M. Lytvyn, V.P. Ovsyannikov, E.A. Mazurenko, Zinc oxide—analogue of GaN with new perspective possibilities, Cryst. Res. Technol. 39 (2004) 980–992.
[22] D.C. Look, New developments in ZnO materials and devices, in: F.H. Teherani, C.W. Litton (Eds.), Zinc Oxide Materials and Devices II, Proc. SPIE 6474 (2007) 647402.
[23] Q.H. Li, Y.X. Liang, Q. Wan, T.H. Wang, Oxygen sensing characteristics of individual ZnO nanowire transistors, Appl. Phys. Lett. 85 (2004) 6389–6391.
[24] J.S. Kim, J. Korean Phys. Soc. 49 (4) (2006) 1635.
[25] O. Lupan, L. Chow, G. Chai, B. Roldan, A. Naitabdi, A. Sculte, H. Heinrich, Nanofabrication and characterization of ZnO nanorod arrays and branched microrods by aqueous solution route and rapid thermal processing, Mater. Sci. Eng. B 145 (2007) 57–66.
[26] L. Schmidt-Mende, J. MacManus-Driscoll, ZnO-nanostructures, defects, and devices, Mater. Today 10 (2007) 41–48.
[27] O. Lupan, L. Chow, G. Chai, A. Schulte, S. Park, O. Lopatiuk-Tirpak, L. Chernyak, H. Heinrich, Biopolymer-assisted self-assembly of ZnO nanoarchitectures from nanorods, Superlattice Microst. 43 (4) (2008) 292–302.
[28] O. Lupan, L. Chow, G. Chai, H. Heinrich, Fabrication and characterization of Zn-ZnO core-shell microspheres from nanorods, Chem. Phys. Lett. 465 (2008) 249–253.
[29] J. Huh, G.-T. Kim, J.S. Lee, S. Kim, A direct measurement of the local resistances in a ZnO tetrapod by means of impedance spectroscopy: the role of the junction in the overall resistance, Appl. Phys. Lett. 93 (2008) 042111.
[30] M.C. Newton, S. Firth, P.A. Warburton, ZnO tetrapod Schottky photodiodes, Appl. Phys. Lett. 89 (2006) 072104.
[31] Y. Cui, U. Banin, M.T. Bjork, A.P. Alivisatos, Electrical transport through a single nanoscale semiconductor branch point, Nano Lett. 5 (2005) 1519–1523.
[32] M.C. Newton, S. Firth, P.A. Warburton, Photoresponse of ZnO tetrapod nanocrystal Schottky diodes, IEEE Trans. Nanotechnol. 7 (2008) 20–23.
[33] Z. Zhang, Li. Sun, Y. Zhao, Z. Liu, D. Liu, L. Cao, B. Zou, W. Zhou, C. Gu, S. Xie, ZnO tetrapods designed as multiterminal sensors to distinguish false responses and increase sensitivity, Nano Lett. 8 (2008) 652–655.
[34] O. Lupan, L. Chow, G. Chai, A. Schulte, S. Park, H. Heinrich, A rapid hydrothermal synthesis of rutile SnO_2 nanowires, Mater. Sci. Eng. B 157 (2009) 101–104.
[35] L. Chow, O. Lupan, H. Heinrich, G. Chai, Self-assembly of densely packed and aligned bilayer ZnO nanorod arrays, Appl. Phys. Lett. 94 (2009) 163105.
[36] C.Y. Yeh, Z.W. Lu, S. Froyen, A. Zunger, Zinc-blende–wurtzite polytypism in semiconductors, Phys. Rev. B 46 (1992) 10086.
[37] R.W.G. Wyckoff, Crystal Structure, vol. 1, 2nd ed., Interscience, New York, 1963.
[38] E. Parthe, Crystal Chemistry of Tetrahedral Structures, Gordon and Breach, New York, 1964.
[39] D.J. Milliron, S.M. Hughes, Y. Cui, L. Manna, J. Li, L.-W. Wang, A. Paul Alivisatos, Colloidal nanocrystal heterostructures with linear and branched topology, Nature 430 (2004) 190–195.

[40] Y. Ding, Z.L. Wang, T. Sun, J. Qiu, Zinc-blende ZnO and its role in nucleating wurtzite tetrapods and twinned nanowires, Appl. Phys. Lett. 90 (2007) 153510.
[41] M. Bender, E. Fortunato, P. Nunes, I. Ferreira, A. Marques, R. Martins, N. Katsarakis, V. Cimalla, G. Kiriakidis, Highly sensitive ZnO ozone detectors at room temperature, Jpn. J. Appl. Phys. 42 (2003) L435–L437.
[42] M.S. Arnold, P. Avouris, Z.W. Pan, Z.L. Wang, Field-effect transistors based on single semiconducting oxide nanobelts, J. Phys. Chem. B 107 (3) (2003) 659–663.
[43] Q.H. Li, Q. Wan, Y.X. Liang, T.H. Wang, Electronic transport through individual ZnO nanowires, Appl. Phys. Lett. 84 (2004) 4556.
[44] J.I. Pankove, Optical Processes in Semiconductors, Prentice Hall, New York, 1971, p. 305.
[45] E. Monroy, F. Calle, J.L. Pau, F.J. Sanchez, E. Munoz, F. Omnes, B. Beaumont, P. Gibart, Analysis and modeling of $Al_xGa_{1-x}N$-based Schottky barrier photodiodes, J. Appl. Phys. 88 (2000) 2081.
[46] V. Henrich, P.A. Cox, The Surface Science of Metal Oxides, Cambridge University Press, Cambridge, 1996.
[47] V.E. Henrich, The Surface Science of Metal Oxides, Cambridge University Press, New York, 1994.

Biographies

Oleg Lupan received his M.S. in microelectronics and semiconductor devices from the Technical University of Moldova (TUM) in 1993. He received his Ph.D. in solid state electronics, microelectronics and nanoelectronics from the Institute of Applied Physics, Academy of Sciences of Republic of Moldova in 2005. He is a visiting professor and researcher at the Department of Physics, University of Central Florida, USA. He is an associate professor (from 2008) and researcher scientist (from 1994) in solid state electronics, microelectronics and nanoelectronics at the Department of Microelectronics and Semiconductor Devices of the Technical University of Moldova (TUM). His current research interests range over semiconducting oxides micro-nanoarchitectures and thin films for chemical sensors, optoelectronic devices and solar cells; nanotechnologies with self-assembly, chemical and electrochemical depositions; development and investigation of novel micro-nanodevices.

Lee Chow is the associate chair and professor of the Department of Physics, University of Central Florida, Orlando. He received his B.S. in physics in 1972 from the National Central University, Taiwan. He received Ph.D. in physics from Clark University, Worcester, MA, USA in 1981. In 1981–1982 he was postdoc in physics at the University of North Carolina, Chapel Hill, NC. He joined the University of Central Florida in 1983 as an assistant professor, and was promoted to associate professor in 1988, and to professor in 1998. Areas of expertise: chemical bath deposition, nanofabrications of carbon nanotubes and metal oxide architectures, diffusion in semiconductors, high T_c thin film, hyperfine interactions, high pressure physics, thin films.

Guangyu Chai is the research director at Apollo Technologies, Inc., Orlando, FL, USA. He received his B.S. in physics in 1999 from the Peking University, Beijing, China. He received Ph.D. in condensed matter physics from University of Central Florida, Orlando, FL, USA in 2004. Research interest: ZnO nanorod sensors; individual carbon nanotube devices, focused ion beam fabrication of nanodevices.